مجلة اكاديمية الجبل للعلوم الاساسية والتطبيقية

Al-Jabal Academy Journal of Pure and Applied Sciences

02 (1): 34-41, 2023

pISSN: 2958-857X; eISSN: 2958-8588

Journal Homepage: https://lajak.edu.ly/journals/index.php/aajpas/index

Investigating the sensing depth of rg405 flat-ended sensor at low microwave frequencies

Mabrouka Haiba A. Ehtaiba[1*]

[1]*Department of Electrical and Electronics Engineering, Sirte University, Sirte, Libya*

DOI: https://doi.org/10.58309/aajpas.v2i1.40

KEYWORDS:

RG405 open-ended coaxial probe, Sensing depth, Reflection coefficient, Low microwave frequencies, Contrast examination.

A B S T R A C T:

Based on the high contrast in the dielectric properties of different tissue types at microwave frequencies, the minimum detectable distance of RG405 flat open-ended coaxial probe is examined using a two-layer structure of different dielectric properties. Since the penetration depth of the scattered electric field produced at the probe aperture is a function of dielectric properties and frequency, the probe performance is tested and verified by carrying out simulations of the fields near the probe for different measurement configurations and intended to illustrate the impact of other materials on the field patterns which ultimately influence the reflection coefficient calculations. Using EMPro software, S_{11} values were computed for the coaxial probe placed against a layered medium with both lossless and lossy phantom experiments. A noticeable contrast is obtained even with two different low lossless materials at 0.1GHz to 3GHz.

التحقق من عمق الإستشعار للمستشعر RG405 ذو النهاية المسطحة عند ترددات الميكروويف المنخفضة

مبروكة هيبة علي احطيبة[1]

قسم الهندسة الكهربائية والإلكترونية، جامعة سرت، سرت، ليبيا

الكلمات المفتاحية:

المستشعر المحوري ذو النهاية المستوية والمفتوحة، ترددات الميكروويف المنخفضة، عمق الإستشعار، فحص التباين، معامل الإنعكاس.

المستخلص:

استنادًا إلى التباين الكبير في خصائص العزل الكهربائي لأنواع الأنسجة المختلفة عند ترددات الميكروويف ، سيتم فحص الحد الأدنى للمسافة التي يمكن اكتشافها بواسطة المستشعر المحوري**RG405** ذو النهاية المستوية والمفتوحة كهربائياً عن طريق طبقتين ذات خصائص عزل كهربائية مختلفة. نظرًا لأن عمق الاختراق للمجال الكهربائي المتناثر الناتج في فتحة المستشعر هو دالة بالنسبة لخصائص العزل الكهربائي والتردد ، سوف يتم اختبار أداء المستشعر والتحقق منه عن طريق إجراء محاكاة للمجالات الكهرومغناطيسية القريبة من النهاية المفتوحة للمستشعر لعدة قياسات مختلفة، ويهدف هذا إلى توضيح تأثير المواد مختلفة الخصائص الكهربائية على أنماط المجال التي بالنتيجة تؤثر على حساب معامل الإنعكاس. قيم معاملات الانعكاس للمستشعر المحوري الموضوع داخل وسط على شكل طبقات سوف يتم حسابها عندما تكون النهاية نماذج لمواد عازلة ومواد موصلة كهربائياً عن طريق برنامج **EMPro**. تباين ملحوظ تم الحصول عليه حتى مع مواد قليلة الفقد عند ترددات من 0.1 إلى 3 قيقاهيرتز.

*Corresponding author:E-mail addresses: ehtaiba.m@su.edu.ly

INTRODUCTION

In the last few years, based on dielectric spectroscopy, there has been a rising interest in developing methodologies for non-invasive electromagnetic diagnostics, particularly operating at microwave frequency bands. Dielectric property has been used for different quality control purposes; such, measurements of the complex dielectric permittivity, ε*(f), have been utilised for a non-destructive broad-band permittivity measurement method (Cataldo et al., 2010) using open-ended coaxial lines terminated by a semi-infinite medium called impedance sensors. In practice, the complex reflection coefficient Γ* is measured by using a network analyzer, afterwards, a model expresses the probe's tip complex admittance as a function of the dielectric permittivity of the surrounding medium and is used to compute ε*.

Open-ended coaxial lines have been utilized as sensors to measure the dielectric properties of biological substances in vivo and in-vitro (Athey et al., 1982; Burdette et al., 1980). For hyperthermia treatments, it is required to precisely determine the dielectric properties of specific human tissues at microwave frequencies. The essential constituents of human tissues are water, free ions such as K+, Cl-, Na+, Ca++, and a variety of proteins. Berube et al., have stated that the dielectric properties of the tissues are similar to those of saline solutions. These types of solutions are characterized by a significant dielectric loss factor at less than 3 GHz (Berube et al., 1996). In addition, these sensors have gained increasing attention for the early detection of cancer by measuring dielectric properties and discriminating tumors from normal tissues, such as the breast (Cheng & Fu, 2018), lymph nodes (Yu et al., 2020), and brain (Gavdush et al., 2020). Recent research presented numerically skin cancer with different sizes, in which S parameters were collected with a 2.2 mm open-ended coaxial probe; moreover, it investigated the contrast between malignant tumors and healthy tissues (Aydinalp et al., 2021). Furthermore, the possibility of recognizing skin cancer from measured electrical properties was demonstrated and the sensing depth of the 2.2 mm diameter open-ended coaxial probe was investigated. (Aydinalp et al., 2019) clarified the effect of open-ended coaxial diameter on the penetration depth (Porter et al., 2017) and demonstrated the relationship between the tissue volume and the contribution of that tissue to the measured dielectric properties.

In this paper, the sensing depth of the 1.68 mm diameter open-ended coaxial probe, that is, how far different properties can be detected, was investigated. The sensitivity assessment is achieved with two layers of lossless and lossy phantoms at a low range of microwave frequencies of 0.1-3GHz.

SENSOR MODELLING

The sensitivity investigation has been performed numerically by using EMPro software which is a numerical simulation based on a Finite Element Method (FEM). The probe was modelled from a semirigid 50Ω coaxial line with an outer diameter of 1.68 mm, inner diameter of 0.51 mm and height of 20 mm. Figure (1) shows the side and front sectional view of the coaxial probe. The investigation started with the probe which feeds it from one port by a 50Ω voltage source and the other port is terminated by the material. The whole system that was modelled consists of two parts, i.e., the coaxial probe (sensor) and the sample of material under test (MUT).

Numerically, the input coaxial port transmits an electromagnetic signal into well-known dielectric material through the open-ended coaxial probe; meanwhile, a reflected signal is received by the same probe. Therefore, based on transmission line theory, reflection coefficients are calculated using transmitted and received signals.

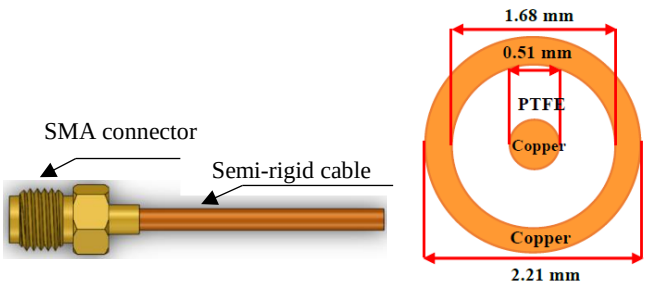

Figure: (1). The front and side sectional views

Sensitivity Examination: The sensitivity of the open-ended coaxial probe was examined with two media with well-known permittivity (air and then deionized water, air and then methanol). Deionized water and methanol were used because their dielectric properties are well-known and high chemical purity samples are easily obtainable. The dielectric constants of pure water and methanol are accurately represented by the Debye equation as expressed in Eq. (1):

$$\varepsilon^* = \varepsilon_\infty + \frac{\varepsilon_s - \varepsilon_\infty}{1 + j\omega\tau} \qquad (1)$$

where ω is the angular frequency. The Debye parameters for pure water and methanol as reported in (Buckley, 1958; by Schwan et al., 2008) are presented in Table (1).

Table:(1). Debye parameters of water and methanol

Parameters		Water	Methanol
ε_s	Static dielectric constant	78.32	34.8
ε_∞	High dielectric constant	4.57	4.5
τ	Characteristic relaxation time	8.38 ps	56 ps

Mosig et al., 1981, presented a solution for the scattering from the open end of a coaxial line in contact with a lossy dielectric, in which the electric field penetration was defined by using the finite element method (FEM). Firstly, The FEM Simulation was carried out with a frequency range (0.1-3 GHz) to compare the effect of different termination samples for the probe at each frequency. The S_{11} complex data for both water and methanol termination was divided by the data for S_{11} when air terminated. Much shorter arcs result on the Smith chart for both liquids, and this will reflect the dielectric property of the material terminating the end.

Sensitivity examination with distance sweep: The sensitivity of the probe was precisely examined in terms of permittivity and frequency with distance sweep, if there are two different layers with different dielectric properties, the probe was injected from the first layer to the other with distance sweep and constant frequency. By helping of simulation first, the experiments were implemented in Empro software to examine their sensitivity with low lossless material (relative permittivity $\varepsilon_r = 1$ and $\varepsilon_r = 3$ respectively). A lossless material has a purely real dielectric constant. After that, layered lossless material (relative permittivity 1 and 10 respectively) Finally, lossy material, fat and muscle tissue layers as human tissues.

The two-layer compositions consisted of a cylindrical size of 5mm radius and 5mm height that was in direct contact with the second cylindric with the same dimensions, but different properties were modelled as illustrated in Figure (2). The probe aperture was injected

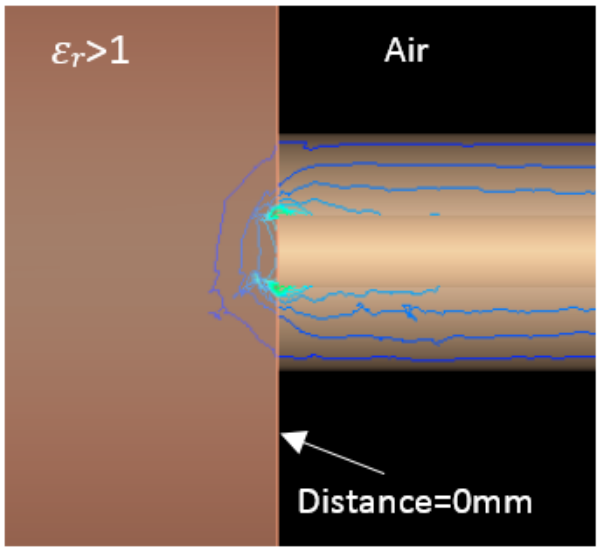

into the first layer to a distance of 1mm away from the interface between the two layers. A numerical distance sweep was done with a total distance of 2mm and, a step of 10μm to estimate the degree to which the sensor can distinguish different samples.

Figure: (2). The two layers with interface region that shows 0mm distance

RESULTS AND DISCUSSION

A comparison shows the clear difference between the relative complex reflection coefficient of water and methanol as shown in Figure (3), which presents that the arcs resulting from the probe are longest for water than methanol, due to the dielectric property of water being higher than methanol as stated in Table (1). Water has more absorption than methanol this explains the significant decrease

in the reflection coefficient for water. Also, as frequency increases the relative complex reflection coefficient decreases in magnitude and phase for both water and methanol. A big contrast can be noticeable between water and methanol, this ensures the capability of the RG405 probe to distinguish water from methanol at low microwave frequencies as expected.

To determine the sensing depth more precisely, two-layer compositions with very low relative permittivity were modelled to test the sensitivity of the probe at 0.1GHz, 0.3GHz, 1GHz, and 3GHz respectively. Air and lossless sample (ε_r = 3) distance sweep for the magnitude of reflection coefficient $|S_{11}|$ are illustrated in Figure (4) (a) at 0.1GHz and 0.3GHz, and Figure (4) (b) at 1GHz and 3GHz respectively.

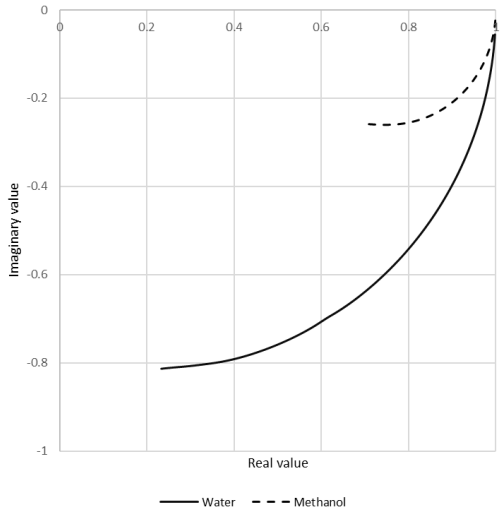

Figure: (3). Relative complex reflection coefficient of water, and methanol

Followed by a plot for the phase of the reflection coefficient as illustrated in Figure (5) (a) at 0.1GHz and 0.3GHz, and Figure (5) (b) at 1GHz and 3GHz respectively. Furthermore, Air and lossless sample (ε_r = 10) distance sweep for the magnitude of reflection coefficient $|S_{11}|$ are illustrated in Figure (6) (a) at 0.1GHz and 0.3GHz, and Figure (6) (b) at 1GHz and 3GHz respectively. Followed by a plot for the phase of the reflection coefficient as illustrated in Figure (7) (a) at 0.1GHz and 0.3GHz, and Figure (7) (b) at 1GHz and 3GHz respectively. The detectable distance increases as frequency increases. It is 0.5mm, 0.2mm, 1.5mm, and 1.2mm for 0.3GHz, 0.1GHz, 3GHz, 1GHz respectively.

When the first layer was in contact with the probe tip which is considered with lower properties, the measured S_{11}'s were essentially those of pure that layer and considered high constant value. However, when the probe tip was moved closer to the second layer which is considered with higher properties, the measurements of S_{11} were linearly related to the compositional fraction of the two materials. As a result of increasing the complex permittivity, the relative complex reflection coefficient decreases. When the probe tip is exactly at the interface between the two layers, the reflection coefficient is dramatically decreased. This is because the whole interaction is with the second layer. In the numerical modelling, slight fluctuations can be noticed in the results which were mainly due to the variations in the mesh density within critical areas for the simulation, e.g., at the centre conductor surface.

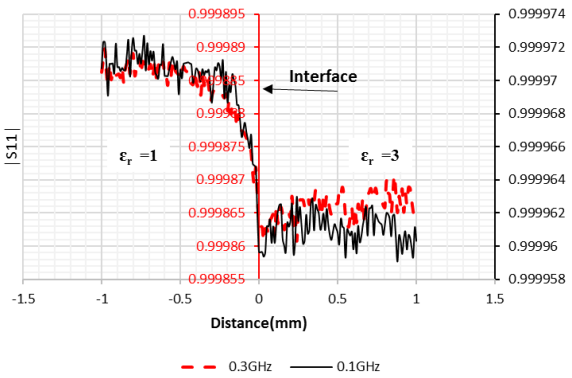

(a)

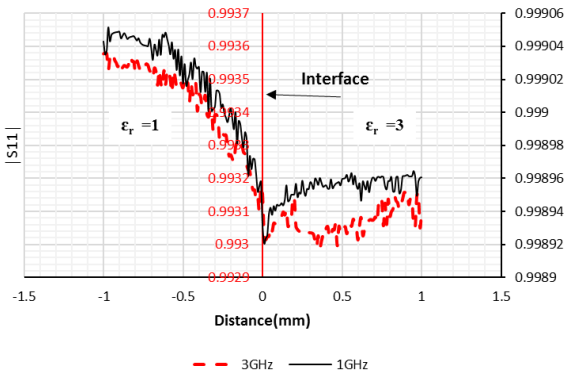

(b)

Figure: (4). The magnitude of reflection coefficient through two layers with ε' = 1 *and* 3, at a)

0.1&0.3GHz, b) 1&3 GHz

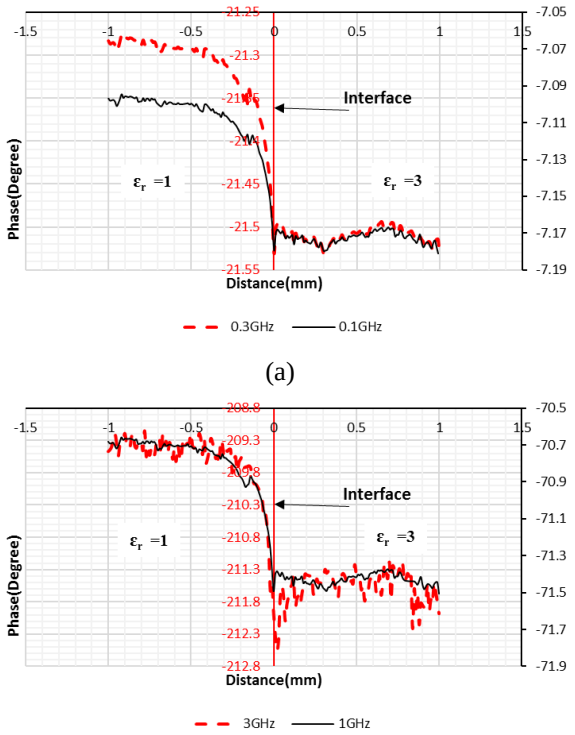

Figure: (5). The phase of reflection coefficient through two layers with ε' = 1 *and* 3, a) at 0.1&0.3GHz, b) at 1&3 GHz

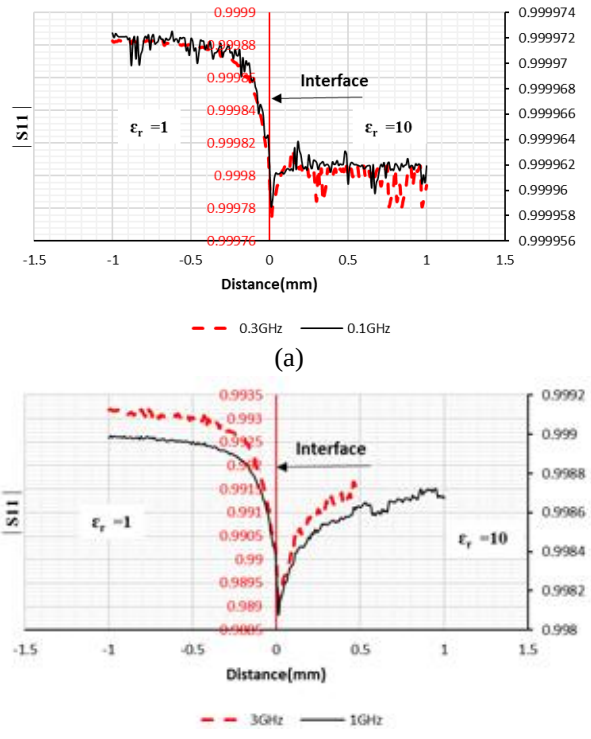

Figure: (6). The magnitude of reflection coefficient through two layers with ε' = 1 *and* 10, a) at 0.1&0.3GHz, b) at 1&3 GHz

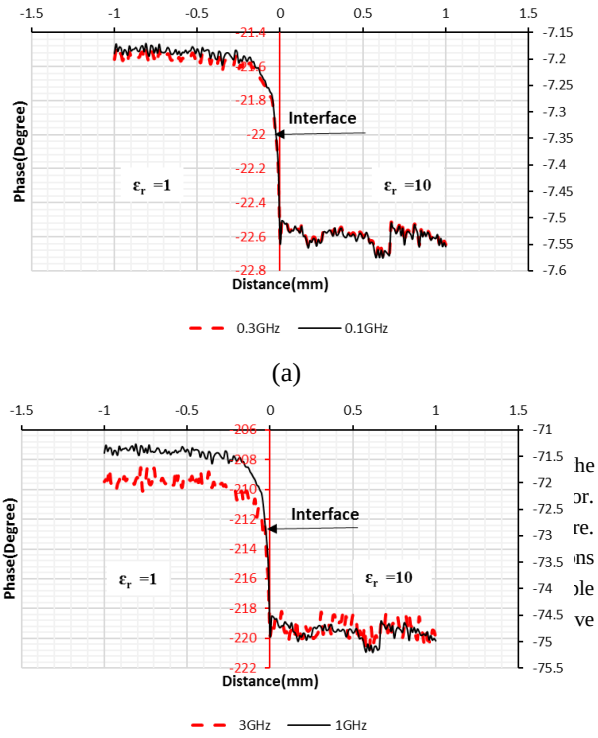

Figure: (7). The phase of reflection coefficient through two layers with ε' = 1 *and* 10, a) at 0.1&0.3GHz, b) at 1&3 GHz

It has been found that the probe was more sensitive for complex reflection coefficient measurements of high-loss media such as water and therefore biological tissues. Figure (8) shows obvious contrast in $|S_{11}|$ when using the probe to detect cylindrical muscle target set at 1mm away from the probe tip at 0.1 GHz, 0.3GHz, 1GHz, and 3GHz. The smallest detecting size is 0.1 mm and 0.4mm for 0.1GHz and 3GHz respectively. Astonishing contrast yielded by phase as illustrated in Figure (9) (a) at 0.1GHz and 0.3GHz, and Figure (9) (b) at 1GHz and 3GHz. These findings clarify the apparent contrast for both phase and $|S_{11}|$ between the fat layer and muscle as the probe moves toward the interface line.

Table (2) shows the relative sensitivity of the probe at different frequency values. It increases as frequency f increases owing to a greater value of $d|S_{11}|/df$.

Table:(2). The probe's relative sensitivity in percentage.
f = 0.1GHz as reference

f(GHz)	Fat		Muscle	
	|S11|%	Phase%	|S11|%	Phase%
0.3	0.13	198.28	0.92	190.41
1	0.71	887.69	2.92	846.66
3	4.06	2838.74	12.21	2629.01

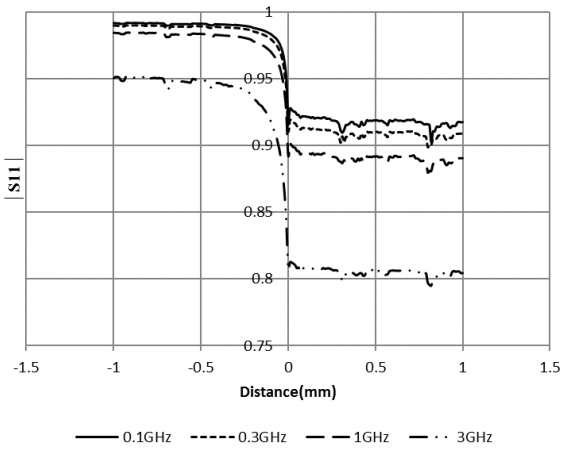

Figure: (8). The magnitude of reflection coefficient through two layers of fat and muscle tissues, at 0.1, 0.3, 1, and 3 GHz

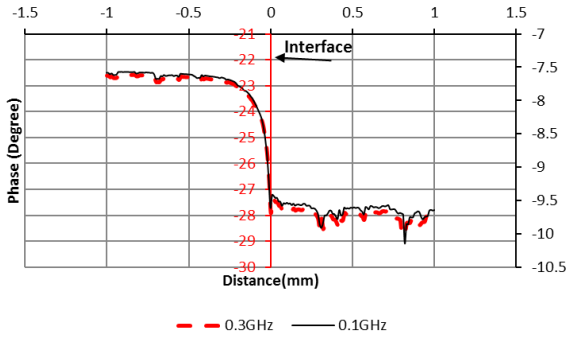

(a)
(b)

Figure: (9). The phase of reflection coefficient through two layers of fat and muscle tissues, a) at 0.1 and 0.3 GHz, b) at 1 and 3 GHz

CONCLUSION

The sensing depth of RG405 open-ended coaxial probe as a function of low microwave frequency and a variety of permittivity has been accomplished numerically. Data from several simple numerical experiments were presented, in which the heterogeneity influence on the reflection coefficients of the sensor is investigated when two layered properties are near the sensor tip. The results suggest that the reflection coefficients are influenced by the material resident within the first 0.1-0.5mm

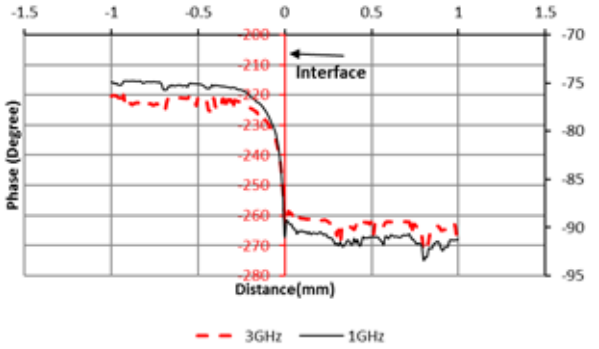

distance from the probe tip. Also, the $|S_{11}|$ and phase values vary with the permittivity and microwave frequency over a frequency range of 0.1 to 3 GHz. Moreover, the findings emphasize the validity of sensitivity improvement for a 1.68mm diameter open-ended coaxial probe and have adequate accuracy at low microwave frequencies for the measurement of low permittivity materials. These results clarify the apparent contrast for both $|S_{11}|$ and phase. However, when measuring low-loss materials, the data of phase are more precise than for $|S_{11}|$. Also, it is observed that the data for the phase are more sensitive to the change of permittivity at a low frequency than the $|S_{11}|$. Based on these findings, phase is quite an appropriate parameter to monitor the contrast at 0.1GHz with the RG405 sensor. Additionally, concerning permittivity, the sensitivity in phase is comparatively high for all the frequencies. Consequently, the phase of the reflection coefficient is suggested to be the most flexible and reliable parameter at low frequency and permittivity. Generally, when characterizing a tissue's electromagnetic properties, the RG405

sensor can be considered the gold standard to provide the ground truth.

ACKNOWLEDGEMENT

Many thanks and gratitude to the Department of Electrical and Electronics Engineering at Sirte University.

GRANT SUPPORT

No specific funding was received for this work.

ETHICS

There are no ethical issues in this manuscript.

REFERENCES

Athey, T. W., Stuchly, M. A., & Stuchly, S. S. 1982. Measurement of Radio Frequency Permittivity of Biological Tissues with an Open-Ended Coaxial Line: Part I. *IEEE Transactions on Microwave Theory and Techniques, 30*(1), 82-86. doi:10.1109/TMTT.1982.1131021

Aydinalp, C., Joof, S., Akduman, I., & Yilmaz, T. (2019, 17-20 *June* 2019). *Sensitivity and Sensing Depth Analysis of Open-ended Contact Probes for Cancer Diagnosis.* Paper presented at the 2019 Photonics & Electromagnetics Research Symposium - Spring (PIERS-Spring).

Aydinalp, C., Joof, S., & Yilmaz, T. (2021, 28 Aug.-4 Sept.). *Microwave Dielectric Property Based Stage Detection of Skin Cancer.* XXXIVth General Assembly and Scientific Symposium of the International Union of Radio Science (URSI GASS) 2021, Rome, Italy

Berube, D., Ghannouchi, F. M., & Savard, P. (1996). A comparative study of four open-ended coaxial probe models for permittivity measurements of lossy dielectric/biological materials at microwave frequencies. *IEEE Transactions on Microwave Theory and Techniques, 44*(10), 1928-1934. doi:10.1109/22.539951

Buckley, F. (1958). *Circular of the Bureau of Standards No. 589: Tables of Dielectric Dispersion Data for Pure Liquids and Dilute Solutions*. Commerce Department, National Institute of Standards and Technology (NIST)

Burdette, E. C., Cain, F. L., & Seals, J. (1980). In Vivo Probe Measurement Technique for Determining Dielectric Properties at VHF through Microwave Frequencies. *IEEE Transactions on Microwave Theory and Techniques, 28*(4), 414-427. doi:10.1109/TMTT.1980.1130087

Cataldo, A., Piuzzi, E., Cannazza, G., De Benedetto, E., & Tarricone, L. (2010). Quality and anti-adulteration control of vegetable oils through microwave dielectric spectroscopy. *Measurement, 43*(8),1031-1039. doi:https://doi.org/10.1016/j.measurement.2010.02.008

Cheng, Y. A.-O., & Fu, M. 2018. Dielectric properties for non-invasive detection of normal, benign, and malignant breast tissues using microwave theories. *Thoracic cancer*, 9(4), 459–465. https://doi.org/10.1111/1759-7714.12605.

Gavdush, A. A., Chernomyrdin, N. V., Komandin, G. A., Dolganova, I. N., Nikitin, P. V., Musina, G. R., Katyba, G. M., Kucheryavenko, A. S., Reshetov, I. V., Potapov, A. A., Tuchin, V. V., & Zaytsev, K. I. 2020. Terahertz dielectric spectroscopy of human brain gliomas and intact tissues ex vivo: double-Debye and double-overdamped-oscillator models of dielectric response. *Biomedical optics express*, 12(1), 69–83. https://doi.org/10.1364/BOE.411025.

Mosig, J. R., Besson, J. E., Gex-Fabry, M., & Gardiol, F. E. (1981). Reflection of an open-ended coaxial line and application to nondestructive measurement of materials. *IEEE Transactions on*

Instrumentation and Measurement, IM-30(1), 46-51. doi:10.1109/TIM.1981.6312437

Porter, E., Gioia, A. L., Elahi, M. A., & Halloran, M. O. (2017, 19-26 Aug. 2017). *Significance of heterogeneities in accurate dielectric measurements of biological tissues.* Paper presented at the 2017 XXXIInd General Assembly and Scientific Symposium of the International Union of Radio Science (URSI GASS).

Schwan, H. P., Sheppard, R. J., & Grant, E. H. (2008). Complex permittivity of water at 25 °C. *The Journal of Chemical Physics, 64*(5), 2257-2258. doi:10.1063/1.432416

Yu, X., Sun, Y. A.-O., Cai, K., Yu, H., Zhou, D., Lu, D., & Xin, S. A.-O. 2020. Dielectric Properties of Normal and Metastatic Lymph Nodes Ex Vivo From Lung Cancer Surgeries. *Bioelectromagnetics*, 41(2), 148–155. https://doi.org/10.1002/bem.22246.